JACS
JOURNAL OF THE AMERICAN CHEMICAL SOCIETY

Article

pubs.acs.org/JACS

Optical Control of Lipid Rafts with Photoswitchable Ceramides

James Allen Frank,[†] Henri G. Franquelim,[‡] Petra Schwille,*[,‡] and Dirk Trauner*[,†]

[†]Department of Chemistry and Center for Integrated Protein Science, Ludwig Maximilians University Munich, Butenandtstraße 5-13, 81377 Munich, Germany

[‡]Department of Cellular and Molecular Biophysics, Max Planck Institute of Biochemistry, Am Klopferspitz 18, 82152 Martinsried, Germany

Supporting Information

ABSTRACT: Ceramide is a pro-apoptotic sphingolipid with unique physical characteristics. Often viewed as a second messenger, its generation can modulate the structure of lipid rafts. We prepared three photoswitchable ceramides, **ACe**s, which contain an azobenzene photoswitch allowing for optical control over the *N*-acyl chain. Using combined atomic force and confocal fluorescence microscopy, we demonstrate that the **ACe**s enable reversible switching of lipid domains in raft-mimicking supported lipid bilayers (SLBs). In the *trans*-configuration, the **ACe**s localize into the liquid-ordered (L_o) phase. Photoisomerization to the *cis*-form triggers a fluidification of the L_o domains, as liquid-disordered (L_d) "lakes" are formed within the rafts. Photoisomerization back to the *trans*-state with blue light stimulates a rigidification inside the L_d phase, as the formation of small L_o domains. These changes can be repeated over multiple cycles, enabling a dynamic spatiotemporal control of the lipid raft structure with light.

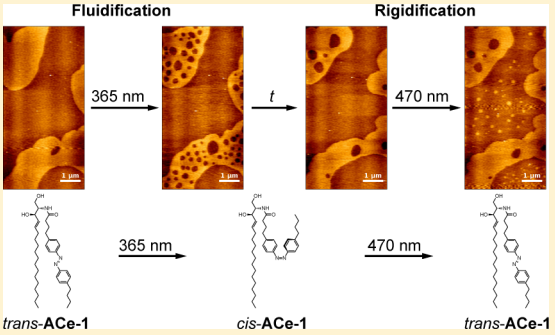

INTRODUCTION

The plasma membrane is not simply a two-dimensional fluid mosaic, but can be laterally organized through the assembly of dynamic lipid domains, the so-called lipid rafts.[1] These segregated domains are thought to permit the two-dimensional organization of membrane components, including both signaling molecules and proteins, leading to the modulation of signaling processes within the plane of the membrane.[2−5] Lipid rafts are structurally and dynamically distinct from the bulk of the lipid bilayer.[5] They are enriched in specific lipid species such as cholesterol (Chol) and sphingolipids.[6,7] Moreover, their physical state is more similar to a liquid-ordered (L_o) phase, in contrast to the rest of the plasma membrane, which is assumed to be mainly in the liquid-disordered (L_d) phase.

While the most abundant sphingolipid in the plasma membrane is sphingomyelin (SM), in recent years the neutral sphingolipid ceramide (Cer) has received great attention for its effects on membrane structure.[8−13] This ubiquitous sphingolipid is often considered a second messenger, and is best known for its role in triggering apoptosis, cell-proliferation, and cell-cycle arrest.[9,14] Defects in Cer metabolism are involved in various disease states.[15] In most healthy cells, Cer concentrations are quite low and tightly regulated. However, its generation via the hydrolysis of SM by sphingomyelinase is stimulated by a variety of cell stress signals or other external factors. This can lead to an overall Cer concentration of 10−20% within the membrane, which has a significant effect on the membrane structure.[9,16] Although structurally similar to diacylglycerol, ceramides possess an elevated melting temperature and are known to rigidify lipid membranes.[17,18] Recent studies in model membrane systems have shown that Cer can trigger the formation of ordered gel-like platforms, and this process is known to be dependent on the length and saturation of its *N*-acyl chain.[19−21]

Currently, chemical tools used to manipulate lipid membranes have failed to address the features of lipid raft and sphingolipid dynamics. For this, a tighter control of individual membrane components must be achieved than with what is currently available.[22] Over the past decades, the emergence of photochemical tools has allowed researchers to translate a light stimulus into a cellular response, with the high degree of spatiotemporal precision associated with light.[23] Caged lipids,[24] whose activities are masked with a photo-labile protecting group, have already proven themselves useful to study lipid signaling at the cellular level.[25,26] In terms of *in vitro* applications, caged ceramides have been shown to modulate lipid domain structure in phase-separated bilayers;[27] yet the effects observed were quite slow and naturally irreversible, as uncaging is a one-shot process.

An alternative approach utilizes photoswitchable small molecules, such as azobenzene derivatives, to translate optical stimuli into a reversible cellular response. This technique has placed a variety of cellular machinery, including ion channels, GPCRs and enzymes, under the control of light.[28] The behavior of photoswitchable azobenzene-modified lipids has been evaluated in model membrane systems before, most notably to explore membrane permeability and surface

Received: July 21, 2016
Published: September 14, 2016

DOI: 10.1021/jacs.6b07278
J. Am. Chem. Soc. 2016, 138, 12981−12986

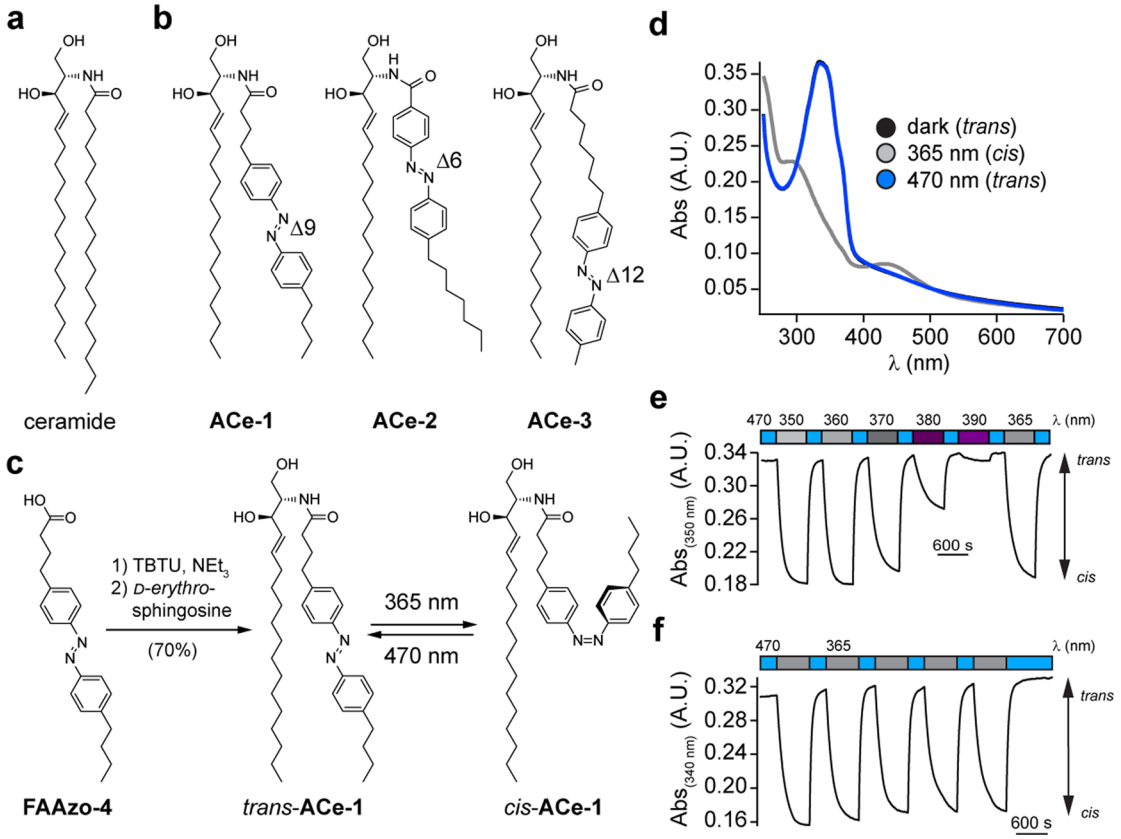

Figure 1. Design and synthesis of photoswitchable ceramides. (a) The chemical structure of C18-ceramide (C18-Cer). (b) The chemical structures of photoswitchable ceramides, **ACe-1**−**3**. (c) D-*erythro*-Sphingosine was converted to the photoswitchable Cer, **ACe-1**, by peptide coupling with **FAAzo-4**. **ACe-1** isomerized between its *cis*- and *trans*-configurations on UV-A (λ = 365 nm) and blue (λ = 470 nm) irradiation, respectively. (d−f) Small unilamellar vesicles containing **ACe-1** (150 μM lipid mixture composed of DOPC:Chol:SM:**ACe-1** 10:6.7:7:3 mol ratio) were analyzed using UV−vis. (d) The spectra of dark- (black), UV- (gray), and blue-adapted (blue) **ACe-1**. The black trace is superimposed under the blue line. (e) **ACe-1** could be isomerized to its *cis*-configuration with UV-A light (λ = 350−380 nm). (f) This effect could be reversed with blue light (λ = 470 nm), and could be repeated over many cycles without fatigue.

pressure.[29−31] Photoswitchable amphiphiles have also been used to enable reversible control of the lipid domain structure in giant unilamellar vesicles.[32,33] However, in those studies, the photoswitch was incorporated into the polar headgroup of the amphiphile, while the membrane-embedded portion remained unaffected by light.

Recently, we developed a series of photoswitchable fatty acids, the **FAAzo**s, which contain an azobenzene photoswitch along the length of the aliphatic chain.[34] The **FAAzo**s can be used as modular building blocks for the construction of more complex photoswitchable lipids, now coined photolipids.[35] Here, we report the incorporation of the **FAAzo**s into the Cer scaffold, which has allowed us to produce, for the first time, a set of intrinsically photoswitchable ceramides, **ACe**s. This approach enables dynamic control over the curvature of the *N*-acyl chain, while still retaining the integrity of the Cer headgroup. Here, we investigate the biophysical properties of this novel class of photolipids within lipid raft-mimicking membrane models using atomic force (AFM) and fluorescence microscopy. In summary, the **ACe**s allow us to restructure, in a reversible manner, ordered lipid domains on isomerization with light.

RESULTS AND DISCUSSION

We designed and synthesized three photoswitchable ceramides, **ACe**s (Figure 1a,b), which are composed of a sphingosine backbone *N*-acylated with one of the **FAAzo**s. **ACe-1**−**3** differ in the position of the azobenzene photoswitch from the near to the distal end of the chain, with the diazene unit representing the Δ9, Δ6, and Δ12 positions, respectively. **ACe-1** was prepared in one step by amide coupling between **FAAzo-4**[31,34] and D-*erythro*-sphingosine in 70% yield (Figure 1c). To investigate the photoswitching behavior in a lipid environment, we incorporated **ACe-1** into small unilamellar vesicles (SUVs) (Figure 1d). In the dark at room temperature, **ACe-1** existed primarily in the thermally stable *trans*-configuration. Irradiation with UV-A light (λ = 350−380 nm) triggered isomerization to the *cis*-configuration (Figure 1e). On termination of the irradiation, **ACe-1** relaxed spontaneously back to the *trans*-form with a τ-value of 39 h, and this effect could be reversed by irradiation with blue light. Photoswitching could be repeated over many cycles without fatigue (Figure 1f). The average size of the SUVs was 66 ± 2 nm, and was not affected by UV-A or blue irradiation, suggesting that the SUVs were stable on photoswitching. **ACe-2** and **ACe-3** were prepared in an analogous fashion by coupling with **FAAzo-1** and **FAAzo-7**, respectively (Figure S1), and possessed similar spectral characteristics when compared to **ACe-1**. As such, the **ACe**s can be described as classical azobenzenes, whose physical orientation can be reversibly modulated by irradiation with UV-A/blue light.

DOI: 10.1021/jacs.6b07278
J. Am. Chem. Soc. 2016, 138, 12981−12986

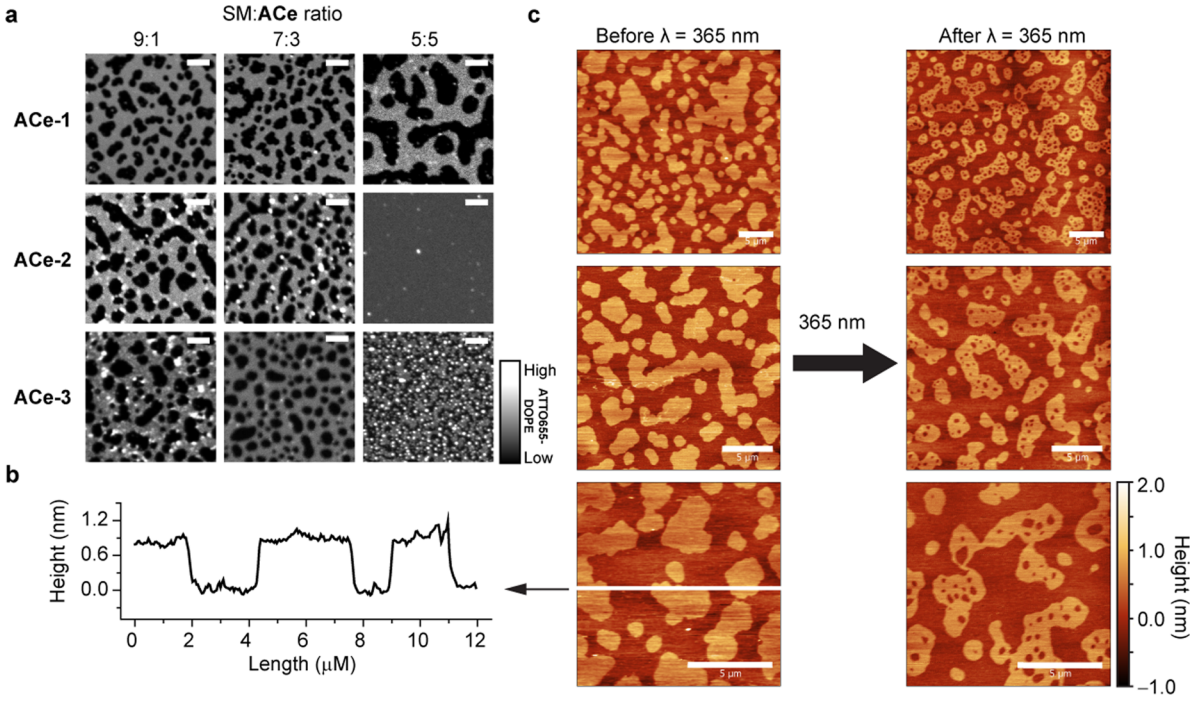

Figure 2. Optical control of ordered lipid domains in supported lipid bilayers (SLBs). (a) Confocal fluorescence images of SLBs containing a quaternary mix of DOPC:Chol:SM:**ACe** (10:6.7:*X*:*Y* mol ratio with 0.1 mol % ATTO655-DOPE). SLBs with SM:**ACe** *X*:*Y* ratios of 9:1, 7:3, and 5:5 are presented for all three **ACe**s. (b) Using atomic force microscopy (AFM), we showed that the ordered (L_o) domains were approximately 0.7−1.1 nm higher than the disordered (L_d) phase in the 7:3 SM:**ACe-1** mixture. (c) Representative AFM images of the 7:3 SM:**ACe-1** mixture showed that isomerization to *cis*-**Ace-1** with λ = 365 nm irradiation triggered the formation of L_d lakes within the L_o domains. Scale bar = 5 μm.

In our previous studies, the effect of different ceramides in L_d−L_o phase separated supported lipid bilayers (SLBs) composed of 1,2-dioleoyl-*sn*-glycero-3-phosphocholine (DOPC), Chol, and C18-SM was investigated.[36,37] Despite the influence of the solid support,[38,39] SLBs provide us with a practical advantage to study both the spatial and topographical properties of such membranes. Using a similar approach, we prepared lipid mixtures containing molar ratios of 10:6.7:*X*:*Y* DOPC:Chol:SM:**ACe** (with 0.1 mol % ATTO655-DOPE for fluorescence detection), and varied the SM:**ACe** (*X*:*Y*) molar ratio between 9:1, 7:3, 5:5, 2.5:7.5, and 0:10 for all three **ACe**s. After deposition of these lipid mixtures on a flat mica surface,[40] we analyzed the resulting SLBs using confocal fluorescence microscopy. We discovered that all three **ACe**s formed ordered domains in the 9:1 and 7:3 SM:**ACe** ratios at room temperature, observed as a decrease in fluorescence intensity in regions of the SLB (Figure 2a). However, at the 5:5 ratio, a difference was observed between the three compounds. The **ACe-1** SLB again formed large ordered domains, whereas **ACe-2** prevented the formation of distinguishable domains, and **ACe-3** formed a bilayer with many small domains, of a structure different from the **ACe-1** SLB. For SM:**ACe** ratios of 2.5:7.5 and 0:10, where minimal or no SM is present, a homogeneous L_d phase was observed for all samples, in accordance with previous studies.[41]

Correlated fluorescence and AFM images in contact mode at room temperature of the 7:3 SM:**ACe-1** mixture confirmed that we had indeed produced a two-phase mixture containing a liquid ordered (L_o) domain, which rested approximately 0.7−1.1 nm above the liquid disordered (L_d) phase (Figure 2b). Similarly, the 9:1 and 5:5 SM:**ACe-1** mixtures possessed identical height profiles. By measuring the depth of holes found within the SLB, we determined a total SLB thickness of 6−7 nm. On irradiation with UV-A light (λ = 365 nm, 10 s), a fluidification of the L_o domains was observed, and small L_d domains (from here-on called "lakes", for the sake of clarity) appeared inside the L_o domains (Figure 2c). The size of the lakes formed within the L_o domains was proportional to the amount of **ACe-1** present in the lipid mixture (Figure S2). In the 9:1 SM:**ACe-1** mixture, only small fluid domains were observed 1 min after UV-A irradiation. After 5 min they had entirely disappeared, presumably via lateral diffusion of lipids into the nearby L_d phase. In contrast, many fluid lakes were formed in the 7:3 and 5:5 SM:**ACe-1** mixtures on UV-A irradiation, and after 5 min most of them had fused to even larger, stable L_d lakes within the L_o domains. In control experiments using C18-Cer, we observed sphingolipid-rich L_o domains that appeared approximately 0.7−1.1 nm above the DOPC-rich liquid disordered (L_d) phase (Figure S3a), and Cer enriched gel-like platforms[37] that were 0.4−1.0 nm higher than the L_o phase (Figure S3b). As expected, the control SLBs containing C18-Cer were not sensitive to UV-A irradiation (Figure S3c). Interestingly, in the case of **ACe-1**, we were never able to observe the presence of a higher gel-like phase, indicating that the formation of such rigid domains may be hindered by the bulkiness of the azobenzene moiety. Using instead a ternary DOPC:SM:**ACe-1** mixture (10:7:3 mol ratio) lacking Chol, we could demonstrate that **ACe-1** allows the formation of gel-like domains (Figure S4), similar to what was reported for C16-Cer.[42] Analogous to our results in the quaternary mixture, on irradiation with UV-A light, a shrinkage of the gel-like domains was observed, as well as small stationary holes within those rigid platforms.

We next utilized high-speed AFM in intermittent-contact mode (AC mode), which allowed us to acquire images of SLBs (quaternary mixtures) at much higher frame rates to facilitate

DOI: 10.1021/jacs.6b07278
J. Am. Chem. Soc. 2016, 138, 12981−12986

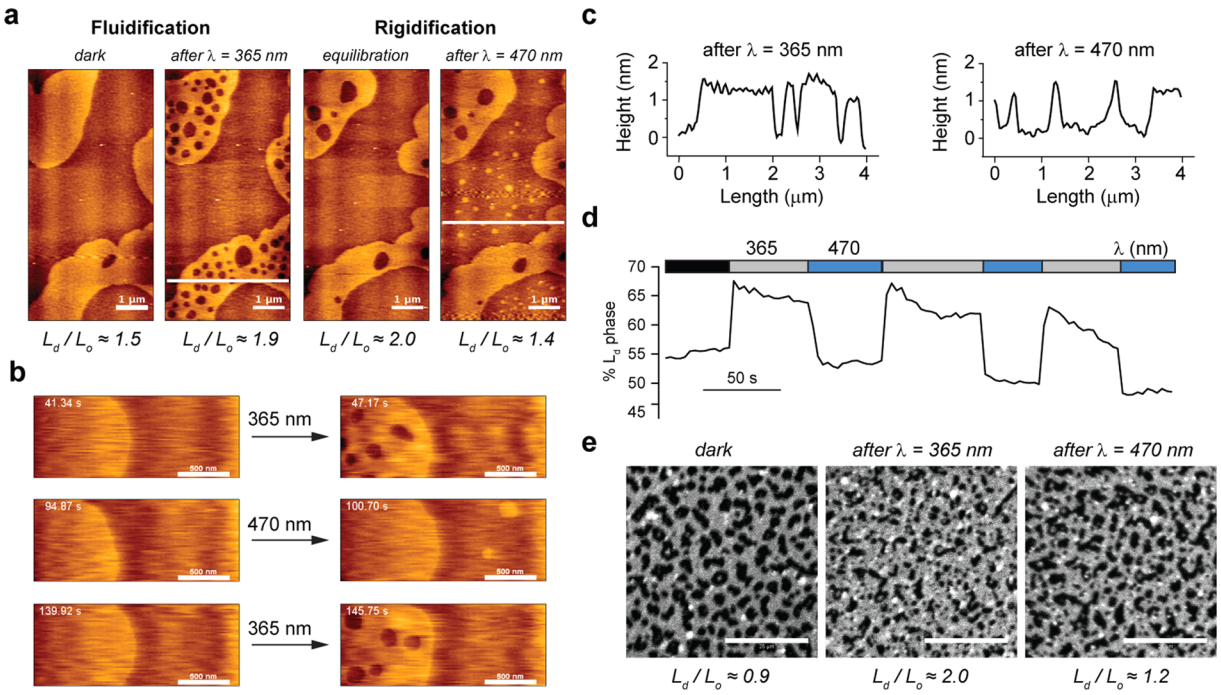

Figure 3. ACe-1 permits reversible remodeling of lipid domains. SLBs containing a DOPC:Chol:SM:**ACe-1** (10:6.7:5:5 mol ratio) lipid mixture were prepared and analyzed using high-speed AFM (AC mode). (a,b) On isomerization to *cis*-**ACe-1**, a fluidification inside the L_o domains was observed as fluid L_d lakes formed within them. On isomerization back to *trans*-**ACe-1** with λ = 470 nm blue light, rigidification was observed within the L_d phase as small L_o islands appeared. (c) Representative height profiles of the membrane (regions marked with white lines in (a)) after irradiation with λ = 365 nm and λ = 470 nm light. (d) Fluidification and rigidification could be repeated over multiple cycles, observed as an increase and decrease in the area of the L_d phase. (e) Using fluorescence confocal microscopy, we could also observe reversible alterations in the SLB domain structure on UV-A/blue irradiation, with an increased L_d/L_o ratio in the *cis*-form.

the observation of domain dynamics on photoisomerization. In the 5:5 SM:**ACe-1** lipid mixture, we were again able to observe the formation of L_d lakes within the L_o phase on isomerization of **ACe-1** from *trans* to *cis* (Figure 3a, left). Immediately after irradiation, the newly formed domains were very small and mobile (Movie S1). They laterally diffused toward the L_d phase, or fused together into larger lakes in an effort to reduce surface tension. After equilibration in *cis*, isomerization back to *trans*-**ACe-1** with blue light (λ = 470 nm) revealed the immediate formation of small L_o rafts within the fluid L_d phase (Figure 3a, right, Figure 3b). The islands were quite small and rested approximately 1.0−1.5 nm higher than the L_d phase (Figure 3c). This height difference is in close agreement with the value obtained for the bilayers under low-speed AFM in contact mode. The small ordered domains quickly disappeared within the first 30 s after blue irradiation, likely due to lipid diffusion into nearby pre-existing L_o domains. By analyzing the fraction of L_d phase as compared to L_o phase (L_d/L_o ratio), we showed that the fraction of L_d increased on UV-A irradiation, while the fraction of L_o increased to similar levels as in the dark-adapted state on blue irradiation (Figure 3a,d). This effect could be repeated over several cycles (Figure 3d, Movie S2), and demonstrates a change in the phase distribution of **ACe-1** within the SLB on isomerization. This effect could also be observed under fluorescence microscopy, confirming that the fluidification was not an artifact caused by the AFM tip (Figure 3e, Figure S5). In this case, the dark L_o domains became smaller, brighter, and less defined on isomerization to *cis*-**ACe-1**. On isomerization back to *trans*-**ACe-1**, the domain structure was slowly restored as the dye diffused out of the ordered domains. For the 7:3 SM:**ACe-1** mixture, the formation of L_o islands within the fluid L_d matrix was also observed on isomerization back to *trans*-**ACe-1**; however, this effect was less prominent when compared to the 5:5 mixture (Figure S6).

Next, we used high-speed AFM to examine different SLB mixtures containing **ACe-2** and **ACe-3** to probe the structure activity relationship between the position of the *N*-acyl azobenzene moiety and the lipid domain structure. In the 7:3 SM:**ACe-2** mixture, only very small and transient L_d lakes were formed inside the L_o domains on isomerization to *cis*-**ACe-2**, while the L_o domains themselves shrunk slightly in size (Figure 4a, Movie S3). Irradiation with blue light reversed this effect, as shown by the L_d/L_o ratio. In comparison, photoswitching of **ACe-3** had a greater effect on the SLB structure. In the 7:3 SM:**ACe-3** mixture, large L_d lakes were observed inside the L_o domains on isomerization to *cis*-**ACe-3**, affording a large increase in the L_d/L_o ratio (Figure 4b, Movie S4). On isomerization back to *trans* with blue light, L_o islands could be observed within the L_d phase, and the ordered domains again grew to their original size.

In the 5:5 SM:**ACe** mixtures, a stark difference was observed between **ACe-2** and **ACe-3**. In agreement with our fluorescence microscopy data, the **ACe-2** mixture formed only a flat fluid phase without domains that was not affected by UV-A irradiation (Figure S7). In the case of **ACe-3**, however, an inversion of the phases was observed. The SLB consisted primarily of a L_o phase, with smaller embedded L_d domains (Figure 4c). Similar to the other lipid mixtures here described, the L_o phase rested 1.0−1.5 nm higher than the L_d domains (Figure 4d). On isomerization to *cis*-**ACe-3**, the L_d domains grew dramatically as the fraction of L_o decreased (Figure 4e). Isomerization back to *trans*-**ACe-3** with blue light reversed this

DOI: 10.1021/jacs.6b07278
J. Am. Chem. Soc. 2016, 138, 12981−12986

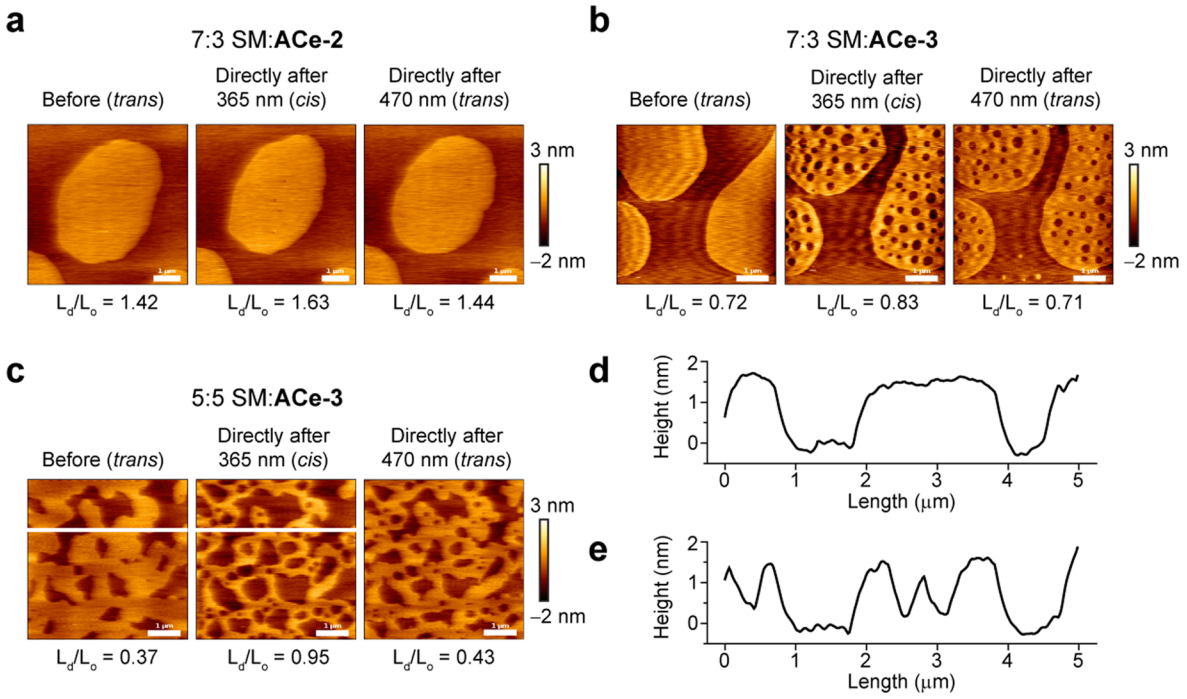

Figure 4. ACe-2 and **ACe-3** enable optical control of ordered lipid domains. SLBs containing DOPC:Chol:SM:**ACe** lipid mixtures (10:6.7:*X*:*Y* mol ratio) were analyzed by high-speed AFM (AC mode). (a) In the 7:3 SM:**ACe-2** mixture, the size of the L_o domains shrunk on isomerization to *cis*-**ACe-2**. Very few L_d lakes were observed within the L_o domains. On isomerization back to *trans*-**ACe-2**, the L_o domains grew to their original size. (b) In the 7:3 SM:**ACe-3** mixture, isomerization had a greater effect on the raft structure, as large L_d lakes and L_o islands were observed on UV-A and blue irradiation, respectively. (c) For the 5:5 SM:**ACe-3** mixture, an inversion of the L_d–L_o phases was observed. As before, UV-A irradiation significantly increased the amount of the L_d phase, while blue irradiation reversed this effect. (d,e) Representative height profiles of the same membrane region (marked with white line) (d) before and (e) after irradiation with λ = 365 nm light. After shining UV-A light, L_d lakes resting approximately 1.0–1.5 nm below the L_o phase can be observed. Scale bar = 1 μm.

effect, and this behavior could be repeated over multiple cycles (Movie S5). These results suggest that **ACe-3** associates itself much more strongly within the L_o domains when compared to **ACe-2**, and consequently a larger difference in raft structure is induced on photoisomerization. It is likely that the location of the azobenzene unit within **ACe-2**, due to its proximity to the headgroup, interferes with the hydrogen bonding between the Cer headgroup and SM. This decreases its presence within the L_o domains, and thus inhibits its efficacy in modulating the architecture of the SLB. In this case, **ACe-2** behaves more like a short-chain Cer derivative,[37] affecting the miscibility and translational order of the L_o domains.[9,43] In contrast, the azobenzene moiety of **ACe-3** is quite far from the headgroup, which permits its incorporation into the L_o lipid rafts in the *trans*-configuration, and thus **ACe-3** behaves more like a long-chain Cer.[37] However, photoisomerization to *cis*-**ACe-3** mimics a bend in the *N*-acyl chain, and disrupts its interactions within the rigid domains. Consequently, this effect triggers **ACe** redistribution into the L_d phase.

CONCLUSION

We demonstrated that **ACe**s in their *trans*-configuration can function similar to Cer in raft mimicking SLBs. Insertion of the hydrophobic azobenzene into the Cer *N*-acyl chain does not inhibit its interaction with L_o domains. Isomerization from the *trans*- to *cis*-configuration induces a conformational change in the fatty acid structure from a less bent (similar to saturated C18:0), to more bent acyl chain (similar to unsaturated C18:1), respectively, allowing us to locally and effectively control the degree of lipid saturation within the bilayer. This result is in accordance with previous studies utilizing the **FAAzo**s,[34] where we demonstrated that they can mimic long and saturated fatty acids in their *trans*-form, whereas they resemble more highly bent fatty acids like arachidonic acid in their *cis*-form. Similar to a previous report investigating the behavior of the unsaturated C18:1-Cer,[44] the bent *cis*-**ACe**s are presumably less soluble within the rigid L_o domains, and therefore prefer to be localized within the fluid phase.

The dynamic manipulation of membrane structure through fluctuations in Cer concentration is thought to be crucial for many biological processes,[16] potentially through the lateral segregation of lipids within the plane of the membrane. *In vitro*, we were able to observe the dynamic formation of small transient ordered domains, alongside the growth of existing ones, on isomerization of the **ACe**s from *cis* to *trans*. As such, the **ACe**s may provide biophysical insights on the requirements necessary to form rigid domains on the membrane on the generation of Cer. Effectively, the **ACe**s permit cycling between ceramides with different biophysical characteristics, enabling dynamic and reversible control over the domain structure within model membranes. This characteristic is not shared with other photochemical tools like caged lipids. We hypothesize that the **ACe**s may become useful to study the role of Cer production in the initiation of apoptosis or other signaling cascades. Furthermore, this work further demonstrates the utility of the **FAAzo**s as modular building blocks that can be used to construct more elaborate photoswitchable sphingolipids. As such, these tools will enable dynamic control over cell membranes, alongside the proteins with which they interact.

DOI: 10.1021/jacs.6b07278
J. Am. Chem. Soc. 2016, 138, 12981–12986

■ ASSOCIATED CONTENT

Supporting Information

The Supporting Information is available free of charge on the ACS Publications website at DOI: 10.1021/jacs.6b07278.

Experimental details for compound synthesis and characterization, as well as SLB formation, and fluorescence and AFM imaging (PDF)

Remodeling of lipid domains by **ACe-1** on a DOPC:Chol:SM:**ACe-1** (10:6.7:5:5) lipid mixture SLB recorded using high-speed AFM (13 s/frame) (AVI)

Remodeling of lipid domains by **ACe-1** on a DOPC:Chol:SM:**ACe-1** (10:6.7:5:5) lipid mixture SLB recorded using high-speed AFM (0.53 s/frame) (AVI)

Remodeling of lipid domains by **ACe-2** on a DOPC:Chol:SM:**ACe-2** (10:6.7:7:3) lipid mixture SLB recorded using high-speed AFM (AVI)

Remodeling of lipid domains by **ACe-3** on a DOPC:Chol:SM:**ACe-3** (10:6.7:7:3) lipid mixture SLB recorded using high-speed AFM (AVI)

Remodeling of lipid domains by **ACe-3** on a DOPC:Chol:SM:**ACe-3** (10:6.7:5:5) lipid mixture SLB recorded using high-speed AFM (AVI)

■ AUTHOR INFORMATION

Corresponding Authors

*schwille@biochem.mpg.de

*dirk.trauner@lmu.de

Notes

The authors declare no competing financial interest.

■ ACKNOWLEDGMENTS

We gratefully acknowledge the Deutsche Forschungsgemeinschaft (SFB 1032) for financial support. D.T. and J.A.F. also acknowledge the European Research Council (ERC Advanced Grant 268795 to D.T.). H.G.F. and P.S. acknowledge the Max Planck Society and the Deutsche Forschungsgemeinschaft (SFB 863) for further support. We thank Margherita Duca and Philipp Blumhardt for experimental assistance. We thank CordenPharma Switzerland (Liestal, CH) for providing lipid starting materials for chemical synthesis.

■ REFERENCES

(1) Simons, K.; Ikonen, E. *Nature* **1997**, *387*, 569.

(2) Rimmerman, N.; Bradshaw, H. B.; Kozela, E.; Levy, R.; Juknat, A.; Vogel, Z. *Br. J. Pharmacol.* **2012**, *165*, 2436.

(3) Simons, K.; Toomre, D. *Nat. Rev. Mol. Cell Biol.* **2000**, *1*, 31.

(4) Simons, K.; van Meer, G. *Biochemistry* **1988**, *27*, 6197.

(5) Brown, D.; London, E. *Annu. Rev. Cell Dev. Biol.* **1998**, *14*, 111.

(6) Eggeling, C.; Ringemann, C.; Medda, R.; Schwarzmann, G.; Sandhoff, K.; Polyakova, S.; Belov, V. N.; Hein, B.; von Middendorff, C.; Schönle, A.; Hell, S. W. *Nature* **2009**, *457*, 1159.

(7) Brown, D. A.; London, E. *J. Biol. Chem.* **2000**, *275*, 17221.

(8) van Blitterswijk, W. J.; van der Luit, A. H.; Veldman, R. J.; Verheij, M.; Borst, J. *Biochem. J.* **2003**, *369*, 199.

(9) Castro, B. M.; Prieto, M.; Silva, L. C. *Prog. Lipid Res.* **2014**, *54*, 53.

(10) Goni, F. M.; Sot, J.; Alonso, A. *Biochim. Biophys. Acta, Biomembr.* **2006**, *1758*, 1902.

(11) Cremesti, A. E.; Goni, F. M.; Kolesnick, R. *FEBS Lett.* **2002**, *531*, 47.

(12) Zou, S.; Johnston, L. J. *Curr. Opin. Colloid Interface Sci.* **2010**, *15*, 489.

(13) Ira; Johnston, L. J. *Langmuir* **2006**, *22*, 11284.

(14) Obeid, L.; Linardic, C.; Karolak, L.; Hannun, Y. *Science* **1993**, *259*, 1769.

(15) Schmuth, M.; Man, M. Q.; Weber, F.; Gao, W.; Feingold, K. R.; Fritsch, P.; Elias, P. M.; Holleran, W. M. *J. Invest. Dermatol.* **2000**, *115*, 459.

(16) Levade, T.; Jaffrézou, J.-P. *Biochim. Biophys. Acta, Mol. Cell Biol. Lipids* **1999**, *1438*, 1.

(17) Holopainen, J. M.; Lehtonen, J. Y. A.; Kinnunen, P. K. J. *Chem. Phys. Lipids* **1997**, *88*, 1.

(18) Holopainen, J. M.; Subramanian, M.; Kinnunen, P. K. J. *Biochemistry* **1998**, *37*, 17562.

(19) Pinto, S. N.; Silva, L. C.; Futerman, A. H.; Prieto, M. *Biochim. Biophys. Acta, Biomembr.* **2011**, *1808*, 2753.

(20) Trajkovic, K.; Hsu, C.; Chiantia, S.; Rajendran, L.; Wenzel, D.; Wieland, F.; Schwille, P.; Brügger, B.; Simons, M. *Science* **2008**, *319*, 1244.

(21) Megha; Sawatzki, P.; Kolter, T.; Bittman, R.; London, E. *Biochim. Biophys. Acta, Biomembr.* **2007**, *1768*, 2205.

(22) Edidin, M. *Annu. Rev. Biophys. Biomol. Struct.* **2003**, *32*, 257.

(23) Velema, W. A.; Szymanski, W.; Feringa, B. L. *J. Am. Chem. Soc.* **2014**, *136*, 2178.

(24) Höglinger, D.; Nadler, A.; Schultz, C. *Biochim. Biophys. Acta, Mol. Cell Biol. Lipids* **2014**, *1841*, 1085.

(25) Shigenaga, A.; Hirakawa, H.; Yamamoto, J.; Ogura, K.; Denda, M.; Yamaguchi, K.; Tsuji, D.; Itoh, K.; Otaka, A. *Tetrahedron* **2011**, *67*, 3984.

(26) Kim, Y. A.; Ramirez, D. M. C.; Costain, W. J.; Johnston, L. J.; Bittman, R. *Chem. Commun.* **2011**, *47*, 9236.

(27) Ramirez, D. M. C.; Pitre, S. P.; Kim, Y. A.; Bittman, R.; Johnston, L. J. *Langmuir* **2013**, *29*, 3380.

(28) Broichhagen, J.; Frank, J. A.; Trauner, D. *Acc. Chem. Res.* **2015**, *48*, 1947.

(29) Fujiwara, H.; Yonezawa, Y. *Nature* **1991**, *351*, 724.

(30) Song, X.; Perlstein, J.; Whitten, D. G. *J. Am. Chem. Soc.* **1997**, *119*, 9144.

(31) Sandhu, S. S.; Yianni, Y. P.; Morgan, C. G.; Taylor, D. M.; Zaba, B. *Biochim. Biophys. Acta, Biomembr.* **1986**, *860*, 253.

(32) Yasuhara, K.; Sasaki, Y.; Kikuchi, J. I. *Colloid Polym. Sci.* **2008**, *286*, 1675.

(33) Hamada, T.; Sugimoto, R.; Nagasaki, T.; Takagi, M. *Soft Matter* **2011**, *7*, 220.

(34) Frank, J. A.; Moroni, M.; Moshourab, R.; Sumser, M.; Lewin, G. R.; Trauner, D. *Nat. Commun.* **2015**, *6*, 7118.

(35) Frank, J. A.; Yuschenko, D. A.; Hodson, D. J.; Lipstein, N.; Nagpal, J.; Rutter, G. A.; Rhee, J.-S.; Gottschalk, A.; Brose, N.; Schultz, C.; Trauner, D. *Nat. Chem. Biol.* **2016**, *12*, 755.

(36) Chiantia, S.; Ries, J.; Chwastek, G.; Carrer, D.; Li, Z.; Bittman, R.; Schwille, P. *Biochim. Biophys. Acta, Biomembr.* **2008**, *1778*, 1356.

(37) Chiantia, S.; Kahya, N.; Schwille, P. *Langmuir* **2007**, *23*, 7659.

(38) Giocondi, M.; Yamamoto, D.; Lesniewska, E.; Milhiet, P.; Ando, T.; Le, C. *Biochim. Biophys. Acta, Biomembr.* **2010**, *1798*, 703.

(39) Alessandrini, A.; Facci, P. *Soft Matter* **2014**, *10*, 7145.

(40) Chiantia, S.; Kahya, N.; Ries, J.; Schwille, P. *Biophys. J.* **2006**, *90*, 4500.

(41) Castro, B. M.; Silva, L. C.; Fedorov, A.; de Almeida, R. F. M.; Prieto, M. *J. Biol. Chem.* **2009**, *284*, 22978.

(42) Castro, B. M.; de Almeida, R. F. M.; Silva, L. C.; Fedorov, A.; Prieto, M. *Biophys. J.* **2007**, *93*, 1639.

(43) Goñi, F. M.; Alonso, A. *Biochim. Biophys. Acta, Biomembr.* **2009**, *1788*, 169.

(44) Pinto, S. N.; Silva, L. C.; de Almeida, R. F. M.; Prieto, M. *Biophys. J.* **2008**, *95*, 2867.

DOI: 10.1021/jacs.6b07278
J. Am. Chem. Soc. 2016, 138, 12981−12986